Visual Coverage Control for Teams of Quadcopters via Control Barrier Functions

Riku Funada[1], María Santos[2], Junya Yamauchi[1], Takeshi Hatanaka[3], Masayuki Fujita[1], and Magnus Egerstedt[2]

***Abstract*— This paper presents a coverage control strategy for teams of quadcopters that ensures that no area is left unsurveyed in between the fields of view of the visual sensors mounted on the quadcopters. We present a locational cost that quantifies the team's coverage performance according to the sensors' performance function. Moreover, the cost function penalizes overlaps between the fields of view of the different sensors, with the objective of increasing the area covered by the team. A distributed control law is derived for the quadcopters so that they adjust their position and zoom according to the direction of ascent of the cost. Control barrier functions are implemented to ensure that, while executing the gradient ascent control law, no holes appear in between the fields of view of neighboring robots. The performance of the algorithm is evaluated in simulated experiments.**

I. INTRODUCTION

An increasing number of visual sensors have been introduced in urban areas and natural environments [1] with the goal of collecting information about events such as natural phenomena [2], security concerns [3] and urban traffic [4]. Although, for some applications, a stationary network of visual sensors may be sufficient to obtain the necessary information [5], [6], [7], [8], aerial robotic swarms represent an adaptable solution for scenarios where the domain to be monitored or the surveillance requirements may vary [9].

Coordinating a group of aerial robots to visually monitor areas of interest can be considered in the context of the coverage problem [10], [11], [12]. Coverage control deals with how to distribute a collection of mobile sensors in a domain such that the features of interest are appropriately monitored by the team. The quality of the surveillance over the objective area is often quantified according to the performance function of the sensors [13], [14], [15]. For multi-camera systems, the problem of visual coverage has been explored both for stationary camera networks [16], [17] and for cameras on teams of quadcopters [18], [19]. In these scenarios, aspects such as lens distortion [17] or camera resolution [18] are usually taken into account when quantifying the coverage performance of the system.

In this paper, we present a visual coverage algorithm for teams of quadcopters equipped with downward facing cameras. Although the scenario is similar to [18], [19], we propose a new locational cost that simultaneously serves two purposes: (a) quantifying the performance of all the cameras, taking into account their lens distortion as in [17]; and (b) reducing the overlap between fields of view of the quadcopters, to expand the surveyed area as much as possible. However, increasing the covered area may result in the appearance of coverage holes, that is, unsurveyed areas in between contiguous agents that significantly degrade the coverage performance [15], [20], [21], [22]. To prevent this unfavorable situation, the proposed algorithm incorporates control barrier functions [23] among agents whose fields of view form triangulations to ensure that no holes appear in between covered areas.

The remainder of the paper is organized as follows: In Section II, we formalize the problem statement. A new locational cost that encodes the coverage performance of the team and minimizes overlaps between the quadcopters' fields of view is introduced in Section III. A distributed control strategy which allows the team to achieve a critical point of the cost by performing an ascent flow is derived in Section III-A. Section IV introduces a control barrier function that ensures that the fields of view of neighboring agents in the team stay connected. The performance of the proposed method is evaluated in simulation in Section V. Section VI concludes the paper.

II. PROBLEM STATEMENT

Consider the scenario illustrated in Fig. 1, where n quadcopters, indexed by $\mathcal{N} = \{1, \cdots, n\}$, are distributed over the 3D Euclidean space with the objective of covering a planar region, hereafter referred to as the *mission space* and denoted as $\mathcal{Q}$. The mission space is a closed and bounded convex set within a planar environment, $\mathcal{E}$. A density function, $\phi : \mathcal{Q} \to \mathbb{R}$, can be used to encode the importance of each point within the mission space such that, the higher the importance, the higher the value of the density function.

Without loss of generality, the world coordinate frame, Σ_w, is chosen to be right-handed, with the XY_w-plane coplanar to $\mathcal{E}$. If we denote the standard basis of Σ_w as $\{\mathbf{e}_x, \mathbf{e}_y, \mathbf{e}_z\}$, then the environment is

$$\mathcal{E} = \{q \in \mathbb{R}^3 \mid \mathbf{e}_z^T q = 0\},$$

*This work was supported by JSPS KAKENHI Grant Number 16J07893 and by ARL through grant DCIST CRA W911NF-17-2-0181.

[1]R. Funada, J. Yamauchi and M. Fujita are with Department of Systems and Control Engineering, Tokyo Institute of Technology, Tokyo 152-8550, Japan funada@fl.ctrl.titech.ac.jp {yamauchi,fujita}@sc.e.titech.ac.jp

[2]M. Santos and M. Egerstedt are with the School of Electrical and Computer Engineering, Georgia Institute of Technology, Atlanta, GA 30332, USA {maria.santos,magnus}@gatech.edu

[3]T. Hatanaka is with Electronic and Information Engineering, Graduate School of Engineering, Osaka University, Osaka, 565-0871, Japan hatanaka@eei.eng.osaka-u.ac.jp

and the quadcopters are naturally restricted to move in the half space $\{q \in \mathbb{R}^3 \mid \mathbf{e}_z^T q > 0\}$.

In order to monitor the environment, each quadcopter is equipped with a downward facing visual sensor. Let Σ_i be the frame of reference of Quadcopter i, $i \in \mathcal{N}$, located at $p_i = [x_i, y_i, z_i]^T$ with respect to Σ_w and with its standard basis being parallel to the basis of the world frame while hovering, i.e., Σ_i not rotated with respect to Σ_w. We assume that the visual sensor is mounted on the quadcopter using a gimbal such that its image plane is always parallel to the XY_i-plane and Z_i is aligned with the optical axis. If we express the image projection according to a perspective projection model [24], then the origin of Σ_i is located at a distance equal to the focal length, λ_i, above the image plane. In this paper, the image plane of all agents is assumed to be circular with radius r.

Each quadcopter can therefore monitor the portion of the mission space $\mathcal{Q}$ in its *field of view*,

$$\mathcal{F}_i = \left\{ q \in \mathcal{E} \;\middle|\; \|q - [x_i, y_i, 0]^T\| \leq r\frac{z_i}{\lambda_i} \right\},$$

which depends on the position of the quadcopter, p_i, and on the zoom level of its visual sensor, determined by the focal length, λ_i.

The objective of this paper is to achieve a spatial allocation of the team and focal length for each agent such that the combination of all the fields of view $\{\mathcal{F}_1, \ldots, \mathcal{F}_n\}$ results in an optimal coverage of the mission space, $\mathcal{Q}$. Let $\mathbf{p}_i = [p_i^T, \lambda_i]^T$ be the state of Quadcopter i. We assume that the movement of the quadcopter can be controlled according to single integrator dynamics,

$$\dot{\mathbf{p}}_i = u_i, \tag{1}$$

which can be converted to reflect the quadcopter's dynamics, e.g. as in [25]. With this consideration, the state of the agents can evolve to satisfy three different aspects of the coverage objective: (a) the areas of higher importance in the mission space need to be monitored closely by the quadcopters, (b) the area covered by the quadcopters should expand as much as possible over the mission space, while ensuring that (c) no space in between fields of view of contiguous robots is left unsurveyed. We encode requirements (a) and (b) through a locational cost to be optimized by the agents, while (c) is enforced through control barrier functions.

III. COVERAGE CONTROL

A natural way of characterizing the coverage performance of a multi-robot team over a domain of interest, $\mathcal{Q}$, is to define a cost function that quantifies the team's collective performance as a function of the quadcopters' states. The quality of surveillance at a point $q \in \mathcal{Q}$ in the field of view $\mathcal{F}_i$ can be quantified using the model in [17],

$$f(\mathbf{p}_i, q) = f_{\text{pers}}(\mathbf{p}_i, q) f_{\text{res}}(\mathbf{p}_i, q), \tag{2}$$

with $f_{\text{pers}}(\mathbf{p}_i, q)$ characterizing the perspective quality,

$$f_{\text{pers}}(\mathbf{p}_i, q) := \frac{\sqrt{\lambda_i^2 + r^2}}{\sqrt{\lambda_i^2 + r^2} - \lambda_i} \left(\frac{z_i}{\|q - p_i\|} - \frac{\lambda_i}{\sqrt{\lambda_i^2 + r^2}} \right),$$

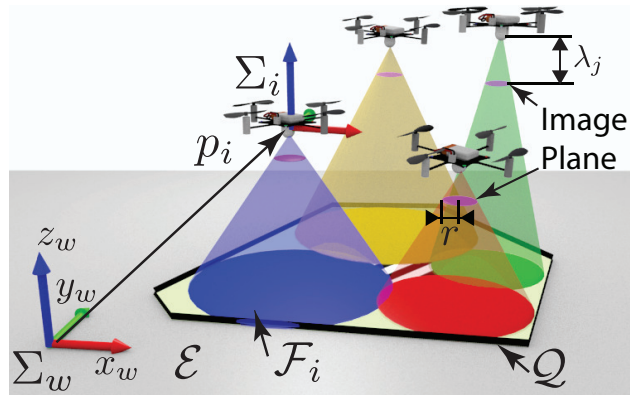

Fig. 1. Proposed scenario. The teams of quadcopters monitor the mission space $\mathcal{Q}$. Agent i's field of view $\mathcal{F}_i$ depends on Agent i's position, p_i, and focal length, λ_i. The crosshatched area among the quadcopters' field of views represents a hole. By using control barrier functions, we will prevent this unsurveyed area from emerging while maximizing the coverage cost.

and $f_{\text{res}}(\mathbf{p}_i, q)$ the loss of resolution,

$$f_{\text{res}}(\mathbf{p}_i, q) := \left(\frac{\lambda_i}{\sqrt{\lambda_i^2 + r^2}} \right)^{\kappa} \exp\left(-\frac{(\|q - p_i\| - R)^2}{2\sigma^2} \right).$$

Analogously to [17], the parameters $\kappa, \sigma > 0$ model the spatial resolution variability of the sensor and $R > 0$ represents the desired range for the vision sensor. If a point is not in the field of view of Quadcopter i, then

$$f(\mathbf{p}_i, q) = 0, \quad q \notin \mathcal{F}_i.$$

Having defined the sensing performance function, the quality of the coverage performed by the quadcopter team can be characterized through the cost,

$$\mathcal{H}_{\mathcal{C}}(\mathbf{p}) = \int_{\mathcal{Q}} \max_{i \in \mathcal{N}} f(\mathbf{p}_i, q)\phi(q)\mathrm{d}q, \tag{3}$$

with a higher value of the cost corresponding to a better coverage of the domain. Here $\mathbf{p} = [\mathbf{p}_1^T, \ldots, \mathbf{p}_n^T]^T$ is the combined state of all the robots and the subscript $\mathcal{C}$ refers to the fact that this cost quantifies the *coverage* quality. Equivalently, if we define the region of dominance of Quadcopter i according to the *conic Voronoi diagram* [17],

$$\mathcal{V}_i(\mathbf{p}) = \{q \in \mathcal{Q} \cap \mathcal{F}_i \mid f(\mathbf{p}_i, q) \geq f(\mathbf{p}_j, q),\ j \in \mathcal{N}\}, \tag{4}$$

the cost in (3) becomes,

$$\mathcal{H}_{\mathcal{C}}(\mathbf{p}) = \sum_{i \in \mathcal{N}} \int_{\mathcal{V}_i(\mathbf{p})} f(\mathbf{p}_i, q)\phi(q)\mathrm{d}q. \tag{5}$$

However, characterizing the coverage performance as in (5) implies that, at a point $q \in \mathcal{Q}$ where several fields of view overlap, only the state of the quadcopter with the best sensing performance at q contributes to the coverage objective. This can be detrimental for the team since those quadcopters with a suboptimal coverage of q could potentially cover alternative areas of the mission space. Let us denote the area covered by Quadcopter i where another quadcopter in the team has a superior sensing performance as

$$\bar{\mathcal{V}}_i(\mathbf{p}) = \{q \in \mathcal{Q} \cap \mathcal{F}_i \mid f(\mathbf{p}_i, q) < f(\mathbf{p}_j, q),\ j \in \mathcal{N}\}.$$

Then, the performance loss caused by the area *overlap* can be quantified as

$$\mathcal{H}_{\mathcal{O}}(\mathbf{p}) = \sum_{i\in\mathcal{N}} \int_{\bar{\mathcal{V}}_i(\mathbf{p})} f(\mathbf{p}_i, q)\phi(q)\mathrm{d}q. \tag{6}$$

We are interested in minimizing the cost in (6) since it characterizes the loss of performance caused by the overlaps among the fields of view. Therefore, we can encode the overall objective combining (6) with (5) as follows,

$$\mathcal{H}(\mathbf{p}) = \mathcal{H}_{\mathcal{C}}(\mathbf{p}) - \mathcal{H}_{\mathcal{O}}(\mathbf{p}), \tag{7}$$

with a higher value of $\mathcal{H}$ corresponding to a better performance of the team under the specified objectives.

A. Gradient Ascent

Having defined a locational cost that characterizes the performance of the team, a natural way to maximize it is to make the quadcopters follow a direction of ascent, that is,

$$\dot{\mathbf{p}}_i = \frac{\partial \mathcal{H}(\mathbf{p})}{\partial \mathbf{p}_i}^T, \quad i \in \mathcal{N}.$$

In order to compute the gradient of (7), let us first consider the gradient of $\mathcal{H}_{\mathcal{C}}$ by applying Leibniz integral rule [26],

$$\frac{\partial \mathcal{H}_{\mathcal{C}}(\mathbf{p})}{\partial \mathbf{p}_i} = \int_{\mathcal{V}_i} \frac{\partial f(\mathbf{p}_i, q)}{\partial \mathbf{p}_i}\phi(q)\mathrm{d}q \tag{8}$$

$$+ \int_{\partial\mathcal{V}_i} f(\mathbf{p}_i, q)\phi(q) n_{ij}^T(q) \frac{\partial q}{\partial \mathbf{p}_i}\mathrm{d}q \tag{9}$$

$$+ \sum_{j\in\mathcal{N}_i} \int_{\partial\mathcal{V}_{ij}} f(\mathbf{p}_j, q)\phi(q) n_{ji}^T(q) \frac{\partial q}{\partial \mathbf{p}_i}\mathrm{d}q, \tag{10}$$

where $\mathcal{N}_i$ are the neighbors of i with respect to the partition in (4),

$$\mathcal{N}_i = \{j \in \mathcal{N} \mid f(\mathbf{p}_i, q) = f(\mathbf{p}_j, q),\ q \in \mathcal{Q}\}, \tag{11}$$

and $\partial\mathcal{V}_i$ and $\partial\mathcal{V}_{ij}$ denote the whole boundary of $\mathcal{V}_i$ and those parts of the boundary shared with Quadcopter j, respectively. We have dropped the dependency of $\mathcal{V}_i$ and its boundaries on $\mathbf{p}$ for notational convenience.

The term in (9) corresponds to a line integral whose domain of integration, $\partial\mathcal{V}_i$, can be composed of

1) boundaries resulting from the overlap of the fields of view of Quadcopter i and other quadcopter's, $\partial\mathcal{V}_{ij}$;
2) segments along the boundary of the mission space, where $\mathcal{V}_i \cap \partial\mathcal{Q}$; and
3) arcs of circumference where $\mathcal{F}_i$ intersects with the interior of the mission space without overlapping with any other agent.

In 1), the terms integrated over $\partial\mathcal{V}_{ij}$ cancel the corresponding term in (10), given that

$$f(\mathbf{p}_i, q) = f(\mathbf{p}_j, q), \quad q \in \partial\mathcal{V}_{ij}, \tag{12}$$

and the normals are opposite to each other, $n_{ij}(q) = -n_{ji}(q)$. For case 2), the term $\partial q/\partial \mathbf{p}_i$ in the integrand is zero, and thus vanishes along those segments. Finally, the sensing performance $f(\mathbf{p}_i, q) = 0$ in the boundary of the field of view, $\mathcal{F}_i$, and, thus, the integrals corresponding to case 3) also become zero. Therefore, the gradient of $\mathcal{H}_C(\mathbf{p}_i)$ is

$$\frac{\partial \mathcal{H}_{\mathcal{C}}(\mathbf{p})}{\partial \mathbf{p}_i} = \int_{\mathcal{V}_i} \frac{\partial f(\mathbf{p}_i, q)}{\partial \mathbf{p}_i}\phi(q)dq.$$

The expression for the derivative of the sensing performance function with respect to the state of Quadcopter i, $\partial f(\mathbf{p}_i, q)/\partial \mathbf{p}_i$, is included in the Appendix.

A similar analysis follows for the gradient of $\mathcal{H}_{\mathcal{O}}$,

$$\frac{\partial \mathcal{H}_{\mathcal{O}}(\mathbf{p})}{\partial \mathbf{p}_i} = \int_{\bar{\mathcal{V}}_i} \frac{\partial f(\mathbf{p}_i, q)}{\partial \mathbf{p}_i}\phi(q)dq.$$

Therefore, the gradient of $\mathcal{H}$,

$$\frac{\partial \mathcal{H}(\mathbf{p})}{\partial \mathbf{p}_i} = \int_{\mathcal{V}_i} \frac{\partial f(\mathbf{p}_i, q)}{\partial \mathbf{p}_i}\phi(q)dq - \int_{\bar{\mathcal{V}}_i} \frac{\partial f(\mathbf{p}_i, q)}{\partial \mathbf{p}_i}\phi(q)dq. \tag{13}$$

Letting Quadcopter i follow a direction of ascent establishes the following coverage theorem.

Theorem 1: Let Quadcopter i, with state $\mathbf{p}_i = [p_i^T, \lambda_i]^T$, evolve according to the control law $\dot{\mathbf{p}}_i = u$, with

$$u = \int_{\mathcal{V}_i} \frac{\partial f(\mathbf{p}_i, q)}{\partial \mathbf{p}_i}^T \phi(q)dq - \int_{\bar{\mathcal{V}}_i} \frac{\partial f(\mathbf{p}_i, q)}{\partial \mathbf{p}_i}^T \phi(q)dq, \tag{14}$$

then, as $t \to \infty$, the quadcopter team will converge to a critical point of the locational cost in (7).

Proof: Let us consider the candidate function

$$V(\mathbf{p}) = U - \mathcal{H}(\mathbf{p}) > 0, \tag{15}$$

with $U = \int_{\mathcal{Q}} \phi(q)\mathrm{d}q$ a strict upper bound of the locational cost, $\mathcal{H}(\mathbf{p})$, given that $f(\mathbf{p}_i, q) \in [0, 1], \forall i \in \mathcal{N}$. Then, the total derivative of (15),

$$\frac{\mathrm{d}V}{\mathrm{d}t} = -\sum_{i\in\mathcal{N}} \frac{\partial \mathcal{H}}{\partial \mathbf{p}_i}\dot{\mathbf{p}}_i = -\left\| \frac{\partial \mathcal{H}}{\partial \mathbf{p}}^T \right\|^2 \leq 0. \tag{16}$$

For (16) to be zero, we need $\partial\mathcal{H}/\partial\mathbf{p} = 0$, which corresponds to $\dot{\mathbf{p}}_i = 0$. By LaSalle's invariance principle, the team will converge to the largest invariant set contained in the set that satisfies $\partial\mathcal{H}/\partial\mathbf{p} = 0$, i.e. the critical points of the cost (7). ■

IV. CONTROL BARRIER FUNCTIONS

Although the control input (14) allows the quadcopter team to fulfill the two objectives stated in Section II, namely, monitoring important areas with the appropriate resolution and expanding the covered area as much as possible; we need to enforce that no area is left unsurveyed in the middle of monitored areas, as illustrated in Fig. 1. If such an area appears, the fields of view surrounding it will prevent any other member of the team from covering it. Thus, the chance of monitoring a hole once it arises is very small.

In order to analyze the existence of coverage holes, we need to characterize the neighborhood of each agent. Let $\mathcal{G}_{\mathcal{F}}(\mathbf{p})$ denote the graph given by the conic Voronoi partition, with neighborhoods given by (11), and $\mathcal{G}_{\mathcal{P}}(\mathbf{p})$ the power diagram [27] characterized by the weighted distance,

$$d_{\mathcal{P}}(\mathbf{p}_i, q) = \|[q_x, q_y]^T - [x_i, y_i]^T\|^2 - \Delta_i^2,$$

where $\Delta_i = rz_i/\lambda_i$ is the radius of $\mathcal{F}_i$. The graph $\mathcal{G}(\mathbf{p}) = \mathcal{G}_{\mathcal{F}} \cap \mathcal{G}_{\mathcal{P}}$ preserves the edges of the power diagram only between those neighbors whose fields of view overlap. Analogously to other works in sensor networks which use triangulations [28], [29], we concern ourselves with triangular subgraphs [30] of the graph $\mathcal{G}(\mathbf{p})$.

For the remainder of this section, we restrict our attention to the coverage holes that may arise, locally, in between three agents $\{i, j, k\}$, that belong to a triangular subgraph of $\mathcal{G}(\mathbf{p})$.

Definition 1: A closed set $E \subset \mathcal{Q}$ is said to be a *hole*, if it satisfies the conditions

$$(\partial E \cap \partial \mathcal{Q} = \emptyset) \ \cap \ (\mathrm{Int}(E) \cap \mathcal{F}_i = \emptyset, \ \forall i \in \mathcal{N}) \quad (17)$$
$$\cap \ E \in Conv(\{[x_i, y_i], [x_j, y_j], [x_k, y_k]\}),$$

where ∂E and $\partial \mathcal{Q}$ denote the boundaries of E and $\mathcal{Q}$; $\mathrm{Int}(E)$, the interior of E; and $Conv(\cdot)$, the convex hull.

Fig. 2a illustrates a *hole* according to our definition. The goal of this section is to ensure that, if the initial deployment of the quadcopter team does not contain a hole, then no hole will appear as a result of executing an ascent flow. Let us denote as $u_{i,\mathrm{nom}}$ the control law given by (14), then we are interested in finding a control u_i^* that remains as close as the nominal input, $u_{i,\mathrm{nom}}$, while ensuring that no holes appear, which can be done through a control barrier function (CBF) [23]. This can be described as the Quadratic Program (QP):

$$u_i^* = \arg\min_{u_i} \|u_i - u_{i,\mathrm{nom}}\|^2 \quad (18)$$
$$\text{s.t. } c_{i,CBF}(\mathbf{p}_i, u_i) \geq 0,$$

where $c_{i,CBF}(\mathbf{p}_i, u_i) \geq 0$ defines the limitations on u_i such that no holes appear.

Before we investigate the expression for $c_{i,CBF}(\mathbf{p}_i, u_i) \geq 0$, a few concepts related to CBFs need to be introduced. Let us define a closed set $\mathcal{C} \in \mathbb{R}^n$, the set of states that do not incur holes. In addition, we assume that such a set can be expressed as the superlevel set of a barrier function, h, i.e. $\mathcal{C} = \{x \in \mathbb{R}^n \mid h(x) \geq 0\}$, where $h : \mathbb{R}^n \to \mathbb{R}$ is a continuously differentiable function.

Definition 2: ([23] *Definition 5*) Given the control affine system

$$\dot{\mathrm{x}} = f(\mathrm{x}) + g(\mathrm{x})\mathrm{u}, \quad (19)$$

where f and g are locally Lipschitz, $\mathrm{x} \in \mathbb{R}^n$ and $\mathrm{u} \in \mathbb{R}^m$, together with the set $\mathcal{C}$, then the function h is a Zeroing Control Barrier Function (ZCBF) defined on a set $\mathcal{D}$ with $\mathcal{C} \subset \mathcal{D} \subset \mathbb{R}^n$, if there exists an extended class $\mathcal{K}$ function, α, such that

$$\sup_{\mathrm{u} \in U} [L_f h(\mathrm{x}) + L_g h(\mathrm{x})\mathrm{u} + \alpha(h(\mathrm{x}))] \geq 0, \ \forall \mathrm{x} \in \mathcal{D}. \quad (20)$$

$L_f h(\mathrm{x})$ and $L_g h(\mathrm{x})$ are the Lie derivatives of $h(\mathrm{x})$ along $f(\mathrm{x})$ and $g(\mathrm{x})$, respectively.

We can guarantee the forward invariance of the set $\mathcal{C}$ through the following corollary.

Corollary 1: ([23] *Corollary 2*) Given a set $\mathcal{C}$, if h is a ZCBF on $\mathcal{D}$, then any Lipschitz continuous controller $\mathrm{u}(\mathrm{x}) : \mathcal{D} \to U$ such that $L_f h(\mathrm{x}) + L_g h(\mathrm{x})\mathrm{u}(\mathrm{x}) + \alpha(h(\mathrm{x})) \geq 0$ will render the set $\mathcal{C}$ forward invariant.

Given that, in our problem, the quadcopter's dynamics are given by (1), $f = 0_{4\times 1}$ and $g = I_4$, with $0_{n\times m}$ an $n \times m$ zero matrix and I_n the $n \times n$ identity matrix, if we use h_{ijk}^3 as an extended class $\mathcal{K}$ function, the QP can be described as

$$u_i^* = \arg\min_{u_i} (u_i - u_{i,\mathrm{nom}})^T W (u_i - u_{i,\mathrm{nom}}) \quad (21)$$
$$\text{s.t. } \frac{\partial h_{ijk}(\mathbf{p}_i, \mathbf{p}_j, \mathbf{p}_k)}{\partial \mathbf{p}_i}^T u_i + h_{ijk}^3(\mathbf{p}_i, \mathbf{p}_j, \mathbf{p}_k) \geq 0,$$

with $W = \mathrm{diag}(1, 1, 1, w_\lambda)$ under the following assumption.

Assumption 1: From the perspective of Agent i, Agents j and k in the triangulation do not move.

Here, w_λ is introduced to adjust the unit difference between the position p_i and the focal length λ_i. Further, Assumption 1 implies that there is no need to calculate $\frac{\partial h_{ijk}}{\partial \mathbf{p}_j}$ or $\frac{\partial h_{ijk}}{\partial \mathbf{p}_k}$ in order to solve the QP (21) in a distributed manner. Although in reality Agents j and k are indeed moving, they are also preventing to make a hole between them and Agent i, and their speed is low. Therefore, we can assume Agents j, k are not moving with respect to Agent i in order to calculate the CBF conditions.

Formulating a CBF that enforces holes do not appear involves understanding the geometric relationships among the fields of view of the agents. To this end, we will again consider three agents $\{i, j, k\}$, which compose a triangular subgraph of $\mathcal{G}(\mathbf{p})$. The power diagram's boundary between two agents is known as a *radical axis*. We denote the radical axis of the sensing regions $\partial\mathcal{F}_i$ and $\partial\mathcal{F}_j$ as L_{ij} given by

$$A_{ij}(x_i, x_j)x + B_{ij}(y_i, y_j)y + C_{ij}(\mathbf{p}_i, \mathbf{p}_j) = 0, \quad (22)$$

where $A_{ij}(x_i, x_j) := 2(x_j - x_i)$, $B_{ij}(y_i, y_j) := 2(y_j - y_i)$ and $C_{ij}(\mathbf{p}_i, \mathbf{p}_j) := x_i^2 - x_j^2 + y_i^2 - y_j^2 + r\left(\frac{z_j}{\lambda_j} - \frac{z_i}{\lambda_i}\right)$. Without loss of generality, we make the following assumption.

Assumption 2: No pair in $\{\partial\mathcal{F}_i, \partial\mathcal{F}_j, \partial\mathcal{F}_k\}$ contain sensing regions that are concentric. Also, not two axes among $\{L_{ij}, L_{jk}, L_{ki}\}$ are parallel.

Assumption 2 ensures that the radical axes $\{L_{ij}, L_{jk}, L_{ki}\}$ exist and are concurrent. The intersection among the three radical axes, the *radical center*, is denoted as v_{ijk} and its x, y coordinates are written as

$$v_{ijk}^x = \frac{B_{ij}C_{ik} - C_{ij}B_{ik}}{A_{ij}B_{ik} - B_{ij}A_{ik}}, \ v_{ijk}^y = \frac{C_{ij}A_{ik} - A_{ij}C_{ik}}{A_{ij}B_{ik} - B_{ij}A_{ik}}. \quad (23)$$

For notational convenience, we have dropped the dependency of v_{ijk}^x and v_{ijk}^y as well as of A_{ij}, B_{ij}, C_{ij} on $\mathbf{p}_i, \mathbf{p}_j, \mathbf{p}_k$.

Let us introduce a Lemma which shows the relationship between a radical center v_{ijk} and the existence of a hole.

Lemma 1: Suppose that Assumption 2 holds and $\partial\mathcal{F}_i, \partial\mathcal{F}_j, \partial\mathcal{F}_k$ have two distinct intersection points for each pair. Then, if there exists a robot $l \in \{i, j, k\}$ which satisfies $v_{ijk} \in \mathcal{F}_l$, there is no *hole*.

Proof: From [31], there are exactly two possibilities for the location of v_{ijk}: (1) v_{ijk} lies outside three circles $\partial\mathcal{F}_i, \partial\mathcal{F}_j, \partial\mathcal{F}_k$; or (2) v_{ijk} lies on or inside all three circles $\partial\mathcal{F}_i, \partial\mathcal{F}_j, \partial\mathcal{F}_k$. Therefore, under the assumptions made, the statement is equivalent to "if v_{ijk} exists on or inside of all three circles $\partial\mathcal{F}_i, \partial\mathcal{F}_j, \partial\mathcal{F}_k$, then there is no *hole*". We

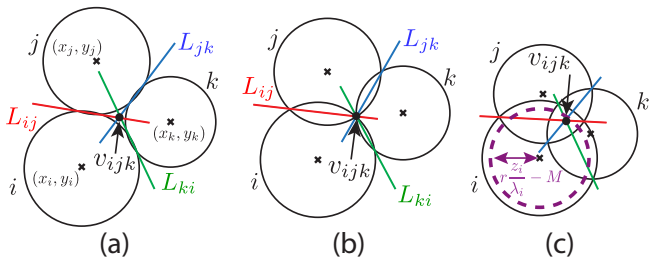

Fig. 2. Three cases of sensing regions deployments. (c) provides intuition about the implemented CBF.

prove this statement by contraposition, namely "if there is a hole, v_{ijk} does not exist on or inside of all three circles $\partial\mathcal{F}_i, \partial\mathcal{F}_j, \partial\mathcal{F}_k$". It is obvious that, if there is a hole, $\mathcal{F}_i \cap \mathcal{F}_j \cap \mathcal{F}_k = \emptyset$. Therefore, $v_{ijk} \notin (\mathcal{F}_i \cap \mathcal{F}_j \cap \mathcal{F}_k)$. This proves the statement. ■

From Lemma 1, we propose the following candidate ZCBF for agent i in order to prevent the formation of holes in the surveyed area,

$$h_{ijk}(\mathbf{p}_i, \mathbf{p}_j, \mathbf{p}_k) = \left(r\frac{z_i}{\lambda_i} - M\right)^2 - \left({V_{ijk}^x}^2 + {V_{ijk}^y}^2\right) > 0, \tag{24}$$

where $V_{ijk}^x = v_{ijk}^x - x_i$, $V_{ijk}^y = v_{ijk}^y - y_i$, and $M > 0$ determines how much overlap is ensured. The interpretation of (24) is to keep v_{ijk} inside of the circle with radius $\left(r\frac{z_i}{\lambda_i} - M\right)$ as depicted in Fig. 2 (c). Since the robot i has the neighbors information, it can calculate (24) in a distributed way. The following lemma shows the effect of the proposed ZCBF on a hole's existence.

Lemma 2: Under Assumption 2, $h_{ijk} > 0$ holds only if $\partial\mathcal{F}_i, \partial\mathcal{F}_j, \partial\mathcal{F}_k$ have two distinct intersection points for each pair and $E = \emptyset$ holds.

Proof: First, we consider the intersection points between robot i and j. It is well known that the power of $P \in L_{ij}$ with respect to $\partial\mathcal{F}_i$ and $\partial\mathcal{F}_j$ take the same value, and the power of P with respect to $\partial\mathcal{F}_i$ is positive if P is outside of $\partial\mathcal{F}_i$, negative if P is inside of $\partial\mathcal{F}_i$ and 0 if $P \in \partial\mathcal{F}_i$. From this property, if $\partial\mathcal{F}_i$ and $\partial\mathcal{F}_j$ do not have any intersection point, then $L_{ij} \cap \mathrm{Int}(\mathcal{F}_i) = \emptyset$ and $L_{ij} \cap \mathrm{Int}(\mathcal{F}_j) = \emptyset$ hold. From $v_{ijk} \in L_{ij}$, if $L_{ij} \cap \mathrm{Int}(\mathcal{F}_i) = \emptyset$, then v_{ijk} never exists in $\mathcal{F}_i$, namely $h_{ijk} \leq 0$. The same is true of agent i and k. Next, we consider agent j and k. If $\partial\mathcal{F}_j$ and $\partial\mathcal{F}_k$ do not have any intersection point, the similar analysis shows that the power of $P \in L_{jk}$ with respect to $\partial\mathcal{F}_j$ and $\partial\mathcal{F}_k$ is always positive. Since the power of three circles at the radical center $v_{ijk} \in L_{jk}$ takes the same value, the power of v_{ijk} with respect to $\partial\mathcal{F}_i$ is also positive. From this fact, v_{ijk} exists outside of $\partial\mathcal{F}_i$. Therefore, $h_{ijk} > 0$ holds only if $\partial\mathcal{F}_i, \partial\mathcal{F}_j, \partial\mathcal{F}_k$ have two distinct intersection points for each pair. It is obvious from (24) that $h_{ijk} > 0$ holds only if v_{ijk} exists inside of $\mathcal{F}_i$. From above discussion and lemma 1, $h_{ijk} > 0$ holds only if $\partial\mathcal{F}_i, \partial\mathcal{F}_j, \partial\mathcal{F}_k$ have two distinct intersection points for each pair and $E = \emptyset$ holds. ■

As the proposed ZCBF ensures that no holes are create, we need to be confirm whether it satisfies Definition 2 and it provides us the forward invariance property.

TABLE I
DENSITY FUNCTION PARAMETERS

Parameter	1	2	3
K_i	3×10^3	2.5×10^3	6×10^2
μ_i	$[0.6, 2.8]^T$	$[3, -0.8]^T$	$[-0.3, 4]^T$
Σ_i	$20\begin{bmatrix}1 & 0.3\\0.3 & 1\end{bmatrix}$	$12\begin{bmatrix}1 & -0.2\\-0.2 & 1\end{bmatrix}$	$8.5\begin{bmatrix}1 & 0.3\\0.3 & 1\end{bmatrix}$

Theorem 2: Suppose that Assumption 2 and $0 < M < \frac{rz_i}{\lambda_i}$ holds. Then, generically, the function h_{ijk} in (24) is a valid ZCBF when $u_i \in \mathbb{R}^4$.

Proof: If $L_g h_{ijk}(\mathbf{p}_i) \neq 0_{4\times1}$ holds, then there exists $u_i \in \mathbb{R}^4$, which satisfies that $L_f h(x) + L_g h(x)u + \alpha(h(x)) \geq 0$ [32]. The derivative of h_{ijk} with respect to $\mathbf{p}_i$ is given by

$$\frac{\partial h_{ijk}}{\partial x_i} = -2\left(V_{ijk}^x\left(\frac{\partial v_{ijk}^x}{\partial x_i} - 1\right) + V_{ijk}^y\frac{\partial v_{ijk}^y}{\partial x_i}\right)$$

$$\frac{\partial h_{ijk}}{\partial y_i} = -2\left(V_{ijk}^x\frac{\partial v_{ijk}^x}{\partial y_i} + V_{ijk}^y\left(\frac{\partial v_{ijk}^y}{\partial y_i} - 1\right)\right)$$

$$\frac{\partial h_{ijk}}{\partial z_i} = 2\frac{r}{\lambda_i}\left(r\frac{z_i}{\lambda_i} - M\right) - 2\left(V_{ijk}^x\frac{\partial v_{ijk}^x}{\partial z_i} + V_{ijk}^y\frac{\partial v_{ijk}^y}{\partial z_i}\right)$$

$$\frac{\partial h_{ijk}}{\partial \lambda_i} = -2\frac{rz_i}{\lambda_i^2}\left(r\frac{z_i}{\lambda_i} - M\right) - 2\left(V_{ijk}^x\frac{\partial v_{ijk}^x}{\partial \lambda_i} + V_{ijk}^y\frac{\partial v_{ijk}^y}{\partial \lambda_i}\right).$$

In general, $\partial h_{ijk}/\partial \mathbf{p}_i = 0$ holds when

$$\frac{rz_i}{\lambda_i} = M. \tag{25}$$

Then, if $0 < M < \frac{rz_i}{\lambda_i}$ holds, $\partial h_{ijk}/\partial \mathbf{p}_i = 0$ never happens except for potential, pathological and non-stationary points. Fig. 2 (c) shows that $\frac{rz_i}{\lambda_i} = M$ only happens when too large a margin M is chosen which is equivalent with Quadcopter i's sensing region. One can easily avoid the condition in (25) by selecting M to be small enough. Thus, we can state that, generically, under an appropriate choice of M, $L_g h_{ijk}(\mathbf{p}_i) \neq 0_{4\times1}$. ■

V. SIMULATION RESULTS

The performance of the proposed algorithm is evaluated through simulation, with a team of 4 quadcopters covering a 12×12 m^2 area. The simulated agents are asked to cover the mission space, $\mathcal{Q}$, depicted in Fig. 4, with respect to the following density function:

$$\phi(q) = 10 + \sum_{i=1}^{3} K_i \exp\left(-\frac{(q-\mu_i)^T\Sigma_i^{-1}(q-\mu_i)}{2}\right), \tag{26}$$

with the parameters given as in Table I.

The control law in (14) is tested in the scenario with and without the ZCBF in Section IV. The parameters for the sensing performance function $f(\mathbf{p}_i, q), \forall i$ are $\kappa = 4$, $R = 3$ and $\sigma = 0.3$, and the parameter for the QP (21) is $w_\lambda = 10^5$.

The evolution of the locational cost in (7) is presented in Fig. 3. In both cases, the distributed gradient ascent algorithm

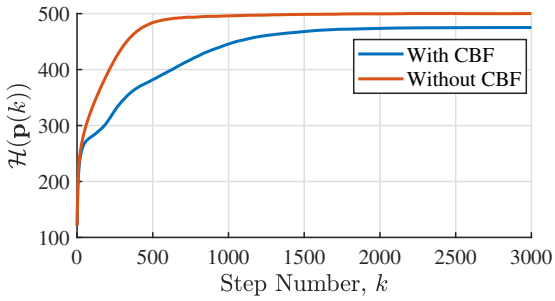

Fig. 3. Comparison of the cost for the experiments in Fig. 4. The price to pay for having a hole-free covered area when using the CBF approach in (21) is slightly smaller than the cost in the final configuration. However, executing the algorithm with the control barrier function ensures that a hole-free area is covered by the quadcopter team at all times.

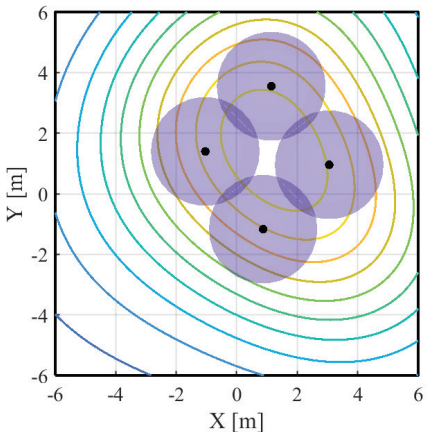

(a) Transient state while using the control law from (14) without the CBF. A hole appears in between the four agents as a result of simply executing gradient ascent, which may be detrimental for the coverage application as the area covered does not remain connected.

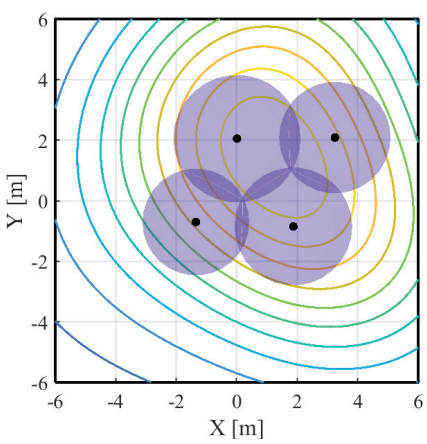

(b) Final state for the proposed algorithm, executing the CBF with the gradient ascent algorithm. As the agents move towards the maximum, no holes appear in between the fields of view. Although the evolution towards the maximum of the cost is slower than in (a) no holes appear.

Fig. 4. Performance of the control law in (14) without (a) and with (b) the zeroing control barrier function.

allows the team to achieve the maximum. We can observe that, in the case of the algorithm with the CBF, the maximum attained is slightly lower than the value achieved for the run without CBFs. However, as shown in Fig. 4, the performance of the gradient ascent with CBF is, usually, superior from a qualitatively point of view, as it ensures that no holes appear in between the agents. In the case of the gradient ascent without CBF, Fig. 4a the coverage is affected by the holes that appear in the middle of the fields of view.

VI. CONCLUSIONS

In this paper, we introduced a visual coverage control algorithm for teams of quadcopters equipped with downward facing cameras. A new locational cost that quantifies the coverage performance of the team was presented in terms of their position and zoom while expanding the area covered by the team as much as possible. However, we observed that, given the limited range of the visual sensors, penalizing the overlaps between the different fields of view may result in the appearance of holes. We proposed a zeroing control barrier function approach to ensure that no holes appear in between the fields of view of neighboring robots. The performance of the algorithm was validated through simulation, showing that, even though the convergence towards the local maximum of the cost is slower for the case of the CBF, we can guarantee that the coverage area has no holes.

APPENDIX

The derivative of the sensing function in (2) with respect to the state of Quadcopter i can be written as,

$$\frac{\partial f}{\partial \mathbf{p}_i} = \frac{\partial f_{\text{pers}}}{\partial \mathbf{p}_i} f_{\text{res}} + f_{\text{pers}} \frac{\partial f_{\text{res}}}{\partial \mathbf{p}_i},$$

where we have suppressed the explicit dependency on $\mathbf{p}_i$ and q for notational convenience.

First, the derivative of $f_{\text{pers}}(\mathbf{p}_i, q)$ with respect to $\mathbf{p}_i = [x_i, y_i, z_i, \lambda_i]^T$ is given by,

$$\frac{\partial f_{\text{pers}}}{\partial x_i} = A(q_x - x_i), \qquad \frac{\partial f_{\text{pers}}}{\partial y_i} = A(q_y - y_i),$$
$$\frac{\partial f_{\text{pers}}}{\partial z_i} = A(q_z - z_i) + \frac{1}{(1-B)\|q - p_i\|},$$
$$\frac{\partial f_{\text{pers}}}{\partial \lambda_i} = \left(\frac{z_i - \|q - p_i\|}{\|q - p_i\|}\right) \frac{r^2}{\sqrt{\lambda_i^2 + r^2}\left(\sqrt{\lambda_i^2 + r^2} - \lambda_i\right)^2},$$

where $q = [q_x, q_y, q_z]^T$ and

$$A = \frac{z_i}{1-B} \frac{1}{\|q - p_i\|^3}, \quad B = \frac{\lambda_i}{\sqrt{\lambda_i^2 + r^2}}.$$

The derivative of $f_{\text{res}}(\mathbf{p}_i, q)$ with respect to $\mathbf{p}_i$,

$$\frac{\partial f_{\text{res}}}{\partial x_i} = C(q_x - x_i), \qquad \frac{\partial f_{\text{res}}}{\partial y_i} = C(q_y - y_i),$$
$$\frac{\partial f_{\text{res}}}{\partial z_i} = C(q_z - z_i),$$
$$\frac{\partial f_{\text{res}}}{\partial \lambda_i} = \frac{\kappa r^2 \lambda^\kappa}{\lambda_i (\lambda_i^2 + r^2)^{\left(\frac{\kappa}{2}+1\right)}} \exp\left(-\frac{(\|q - p_i\| - R)^2}{2\sigma^2}\right),$$

with

$$C = 2B^\kappa \exp\left(-\frac{(\|q - p_i\| - R)^2}{2\sigma^2}\right) \frac{(\|q - p_i\| - R)}{2\sigma^2 \|q - p_i\|}.$$

REFERENCES

[1] X. Wang, "Intelligent multi-camera video surveillance: A review," *Pattern Recognition Letters*, vol. 34, no. 1, pp. 3–19, 2013.

[2] G. Zhou, C. Li, and P. Cheng, "Unmanned aerial vehicle (UAV) real-time video registration for forest fire monitoring," in *Proceedings of 2005 IEEE International Geoscience and Remote Sensing Symposium*, vol. 3, 2005, pp. 1803–1806.

[3] M. M. Trivedi, T. L. Gandhi, and K. S. Huang, "Distributed interactive video arrays for event capture and enhanced situational awareness," *IEEE Intelligent Systems*, vol. 20, no. 5, pp. 58–66, 2005.

[4] S. Srinivasan, H. Latchman, J. Shea, T. Wong, and J. McNair, "Airborne traffic surveillance systems: Video surveillance of highway traffic," in *Proceedings of the ACM 2nd International Workshop on Video Surveillance and Sensor Networks*, 2004, pp. 131–135.

[5] S. Abdurrahman, "Smart video-based surveillance: Opportunities and challenges from image processing perspectives," in *Proceedings of 3rd International Conference on Information Technology, Computer, and Electrical Engineering*, 2016, p. 10.

[6] I. A. K. Mohammed and S. Sasi, "Automated surveillance of unattended bags for complex situations," in *Proceedings of 2009 International Conference on Advances in Computing, Control, and Telecommunication Technologies*, 2009, pp. 850–852.

[7] B. Rinner and W. Wolf, "An introduction to distributed smart cameras," *Proceedings of the IEEE*, vol. 96, no. 10, pp. 1565–1575, 2008.

[8] A. A. Morye, C. Ding, A. K. Roy-Chowdhury, and J. A. Farrell, "Distributed constrained optimization for bayesian opportunistic visual sensing," *IEEE Transactions on Control Systems Technology*, vol. 22, no. 6, pp. 2302–2318, 2014.

[9] S. Chung, A. A. Paranjape, P. Dames, S. Shen, and V. Kumar, "A survey on aerial swarm robotics," *IEEE Transactions on Robotics*, vol. 34, no. 4, pp. 837–855, 2018.

[10] J. Cortes, S. Martinez, T. Karatas, and F. Bullo, "Coverage control for mobile sensing networks," *IEEE Transactions on Robotics and Automation*, vol. 20, no. 2, pp. 243–255, 2004.

[11] C. G. Cassandras and W. Li, "Sensor networks and cooperative control," *European Journal of Control*, vol. 11, no. 4, pp. 436–463, 2005.

[12] S. Martinez, J. Cortes, and F. Bullo, "Motion coordination with distributed information," *IEEE Control Systems Magazine*, vol. 27, no. 4, pp. 75–88, 2007.

[13] A. Pierson, L. C. Figueiredo, L. C. Pimenta, and M. Schwager, "Adapting to sensing and actuation variations in multi-robot coverage," *The International Journal of Robotics Research*, vol. 36, no. 3, pp. 337–354, 2017.

[14] P. Dames, "Distributed multi-target search and tracking using the PHD filter," in *Proceddings of 2017 International Symposium on Multi-Robot and Multi-Agent Systems*, 2017, pp. 1–8.

[15] H. Mahboubi, K. Moezzi, A. G. Aghdam, and K. Sayrafian-Pour, "Distributed deployment algorithms for efficient coverage in a network of mobile sensors with nonidentical sensing capabilities," *IEEE Transactions on Vehicular Technology*, vol. 63, no. 8, pp. 3998–4016, 2014.

[16] M. Forstenhaeusler, R. Funada, T. Hatanaka, and M. Fujita, "Experimental study of gradient-based visual coverage control on SO(3) toward moving object/human monitoring," in *Proceedings of 2015 American Control Conference*, 2015, pp. 2125–2130.

[17] O. Arslan, H. Min, and D. E. Koditschek, "Voronoi-based coverage control of Pan/Tilt/Zoom camera networks," in *Proceedings of 2018 IEEE International Conference on Robotics and Automation*, 2018, pp. 1–8.

[18] M. Schwager, B. J. Julian, M. Angermann, and D. Rus, "Eyes in the sky: Decentralized control for the deployment of robotic camera networks," *Proceedings of the IEEE*, vol. 99, no. 9, pp. 1541–1561, 2011.

[19] S. Papatheodorou, A. Tzes, and Y. Stergiopoulos, "Collaborative visual area coverage," *Robotics and Autonomous Systems*, vol. 92, pp. 126–138, 2017.

[20] N. Boudriga, M. Hamdi, and S. Iyengar, "Coverage assessment and target tracking in 3D domains," *Sensors*, vol. 11, no. 10, pp. 9904–9927, 2011.

[21] R. Ghrist and A. Muhammad, "Coverage and hole-detection in sensor networks via homology," in *Proceedings of 4th International Symposium on Information Processing in Sensor Networks*, 2005, pp. 254–260.

[22] P. K. Sahoo, M.-J. Chiang, and S.-L. Wu, "An efficient distributed coverage hole detection protocol for wireless sensor networks," *Sensors*, vol. 16, no. 3, p. 386, 2016.

[23] A. D. Ames, X. Xu, J. W. Grizzle, and P. Tabuada, "Control barrier function based quadratic programs for safety critical systems," *IEEE Transactions on Automatic Control*, vol. 62, no. 8, pp. 3861–3876, 2017.

[24] Y. Ma, S. Soatto, J. Kosecka, and S. Sastry, *An Invitation to 3-D Vision: From Images to Geometric Models*. SpringerVerlag, 2003.

[25] D. Mellinger and V. Kumar, "Minimum snap trajectory generation and control for quadrotors," in *Proceedings of 2011 IEEE International Conference on Robotics and Automation*, 2011, pp. 2520–2525.

[26] Q. Du, V. Faber, and M. Gunzburger, "Centroidal voronoi tessellations: Applications and algorithms," *SIAM Review*, vol. 41, no. 4, pp. 637–676, 1999.

[27] F. Aurenhammer, "Power diagrams: Properties, algorithms and applications," *SIAM Journal on Computing*, vol. 16, no. 1, pp. 78–96, 1987.

[28] C. Zhu, C. Zheng, L. Shu, and G. Han, "A survey on coverage and connectivity issues in wireless sensor networks," *Journal of Network and Computer Applications*, vol. 35, no. 2, pp. 619–632, 2012.

[29] V. De Silva and R. Ghrist, "Coordinate-free coverage in sensor networks with controlled boundaries via homology," *International Journal of Robotics Research*, vol. 25, no. 12, pp. 1205–1222, 2006.

[30] M. Mesbahi and M. Egerstedt, *Graph Theoretic Methods for Multiagent Networks*. Princeton University Press, 2010.

[31] C. I. Delman and G. Galperin, "A tale of three circles," *Mathematics Magazine*, vol. 76, pp. 15–32, 2003.

[32] X. Xu, P. Tabuada, J. W. Grizzle, and A. D. Ames, "Robustness of control barrier functions for safety critical control," in *Proceedings of IFAC Conference on Analysis and Design of Hybrid Systems*, vol. 48, no. 27, 2015, pp. 54–61.